High-power Soliton-induced Supercontinuum Generation and Tunable Sub-10-fs VUV Pulses from Kagome-lattice HC-PCFs

Song-Jin Im[1,2], Anton Husakou[1], and Joachim Herrmann[1]
[1] *Max-Born-Institute for Nonlinear Optics and Short Pulse Spectroscopy, Max-Born-Str. 2a, D-12489 Berlin, Germany and*
[2] *Natural Science Center, KimIlSung University, Daesong District, Pyongyang, DPR Korea*

We theoretically study a novel approach for soliton-induced high-power supercontinuum generation by using kagome lattice HC-PCFs filled with a noble gas. Anomalous dispersion and broad-band low loss of these fibers enable the generation of two-octave broad spectra by fs pulses, with high coherence and high spectral peak power densities up to five orders of magnitude larger than in standard PCFs. In addition, up to 20% of the output radiation energy forms a narrow UV/VUV band, which can be tuned by controlling the pressure in the range from 350 nm to 120 nm. In the temporal domain this corresponds to sub-10-fs UV/VUV pulses with pulse energy of few tens of μJ, caused by the formation of a high-order soliton emitting non-solitonic radiation.

PACS numbers: 42.65.Re, 42.65.Tg, 42.72.Bj

The discovery of photonic crystal fibers (PCF) had a strong impact on the field of nonlinear fiber optics and led to numerous physical and technological advances and interdisciplinary applications [1]. One of the most interesting type of PCFs is the hollow-core PCF (HC-PCF) [2] in which light is guided in the hollow core via the bandgap in the periodical cladding consisting of a two-dimensional array of air holes. These fibers offer low loss coefficients enabling diverse applications in nonlinear optics. However, the main drawback of these fibers is their intrinsically narrow transmission bandwidth determined by the bandgaps.

An alternative HC-PCF design replaces the triangular lattice of circular air holes with a kagome lattice [see Fig. 1(a)] [3, 4, 5]. The photonic guidance of this fiber is not based on a bandgap but on the inhibited coupling between the core and cladding modes. Due to this guiding mechanism kagome lattice HC-PCFs exhibit broadband transmission with a loss lower than 1 dB/m covering the spectral range from the infrared up to the VUV. These fibers exhibit controlled anomalous dispersion for UV or visible wavelengths both for 1-cell-core as well for 3-ring-core geometries for core diameters in the range of 10 μm to 80 μm [6].

As will be shown in this letter, the combination of broadband transmission and control of zero-dispersion wavelength from visible to UV is of great interest for applications in ultrafast nonlinear optics, especially for a novel type of high-power coherent white light sources (supercontinuum, SC). It is well known that lasers generate high-brightness coherent light only within a restricted bandwidth, while many applications require much broader coherent light with high brightness. A breakthrough in the development of coherent white-light sources was the discovery of two-octave-spanning supercontinuum generation in solid-core PCFs by using femtosecond pulses with only nJ energy from a modelocked laser [7]. The dramatic spectral broadening of low-energy

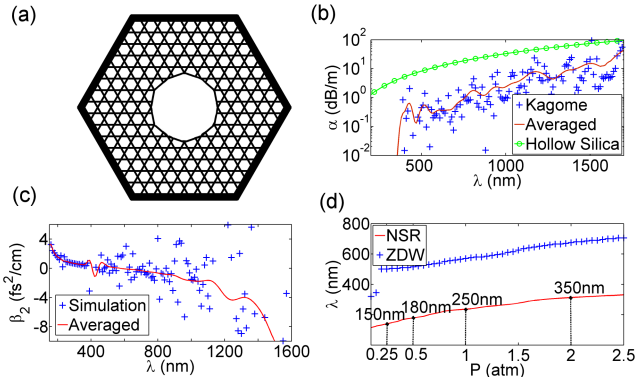

FIG. 1: Cross-section (a), loss (b), GVD (c) and zero-dispersion wavelength (ZDW) and phase-matching wavelength (d) of a 3-ring-core kagome lattice HC-PCF. In (b) and (c), a 3-ring-core kagome lattice HC-PCF with a lattice pitch of 16 μm and a strut thickness of 0.2 μm filled with argon at 1 atm is considered. In (b), the blue crosses represent the direct numerical simulations, the red solid curve is the result after averaging over inhomogenities and the green circles are the loss of a hollow silica waveguide with the same core diameter. In (c), the blue crosses represent the direct numerical simulations and the red solid curve is the averaged results. In (d), the dependence of ZDW (blue crosses) and the phase-matching wavelength (red solid curve) on the gas pressure are presented.

femtosecond pulses in solid-core PCFs significantly differs from previously known spectral broadening mechanisms; it is related to the soliton dynamics in the anomalous-dispersion region of the PCFs [8]. Subsequent experimental studies by many groups provided evidence of this soliton-induced mechanism of SC generation [9, 10, 11], for a review see [12]. Supercontinuum generation from solid-core PCFs plays a key role in a wide range of applications, such as in optical frequency metrology, absorption spectroscopy, optical coherence tomography and biophysics.

Despite the great progress in this field, a significant challenge is to increase the available SC peak power and to extend the spectral broadening into the ultraviolet and vacuum ultraviolet region; advances in this direction are requested by many applications. Unfortunately, the small radii in solid-core PCFs and material damage severely limit the SC peak power densities to tens of W/nm in these fibers. In this paper we propose and theoretically study a novel approach for high-power optical SC generation in argon-filled kagome lattice HC-PCFs. We predict that in such waveguides high-coherence two-octave broad spectra, with up to five orders of magnitude higher spectral peak power densities than in solid-core PCFs, can be generated. It is enabled by three advantages of kagome-lattice argon-filled HC-PCFs: dispersion control by pressure and anomalous dispersion in the visible and UV, large core diameters in the range from 10 μm to 80 μm, and high ionisation threshold of argon. The underlying mechanism differs in an important aspect from that in solid-core PCFs where the supercontinuum arises by the emission of several fundamental solitons. In contrast, in the case of a kagome lattice HC-PCF it arises from a single high-order soliton. The reason for this phenomenon is the absent Raman effect in argon and the low third-order dispersion which leads to a stable propagation of a higher-order soliton over much longer propagation lengths.

A second predicted phenomenon is that the output radiation contains a sub-10-fs UV/VUV pulse which carries about 20% of input energy corresponding to few tens of μJ. The spectrum of this pulse is a narrow-band UV/VUV peak which can be tuned by pressure variation in the range of 350-120 nm. These high-energy VUV pulses can be identified as the non-solitonic radiation from a high-order soliton at the stage of maximum compression that possesses the highest amplitude and the broadest bandwidth. Note that up to now no standard method for the generation of ultrashort pulses in the VUV range exist, and only relatively modest results compared with the progress in the near-infrared spectral range has been achieved, remarkable here is e.g. the generation of 11-fs pulses at 162 nm with 4 nJ energy [13] or 160-fs pulses with a higher energy of 600 nJ at 161 nm [14]. However, ultrashort pulse sources in the UV and VUV spectral range are essential tools in many applications, in particular in time-resolved spectroscopy of molecules, requiring further progress and alternative methods in this field.

Recently, two of the authors studied dielectric-coated metallic hollow waveguides as an option for the generation of high-power high-coherent supercontinua [15]. However, the challenges in the fabrication of these fibers require to proceed with the search for a viable type of hollow waveguides enabling dispersion control and high-power SC generation.

The cross-section of the studied kagome lattice HC-PCF with a 3-ring-core is presented in Fig. 1(a), in which a hollow core filled with a noble gas is surrounded by a kagome lattice cladding and a bulk fused silica outer region. For the calculation of the propagation constant $\beta(\omega)$ and loss $\alpha(\omega)$ of this waveguide the finite-element Maxwell solver JCMwave was utilized [6]. The dispersion of fused silica as well as that of argon was described by the Sellmeyer formula for the corresponding dielectric function. In Fig. 1(b) the loss coefficient is presented which is few orders of magnitude lower than the one of a hollow silica waveguide with the same core diameter, it decreases with decreasing wavelengths and has a magnitude of about 1 dB/m at 800 nm. This low loss is mainly influenced by the strut thickness in the kagome lattice cladding and only weakly depend on the core diameter. We have found that the guiding range of the kagome-lattice HC-PCF in the UV/VUV range is limited only by the loss of argon, while the intrinsic silica loss in the 120-200 nm range does not lead to high waveguide loss.

Figure 1(c) demonstrates the possibility to achieve anomalous GVD at a desired wavelength by choosing a radius smaller than 100 μm. In a real waveguide, there are longitudinal variations of the structure parameters due to manufacturing imperfections, leading to fast longitudinal variation of the propagation constant, which however will be smoothed out during propagation. This smoothing can be also performed in the frequency domain, since the position of the spikes in the loss and dispersion curves scales correspondingly with the varying structure parameters. We assume a 5% variation depth of the inhomogeneity and consider an averaged loss and GVD, as depicted by the red solid curves in Fig. 1(b),(c). In Fig. 1(d) by the blue crosses the dependence of the zero-dispersion wavelength (ZDW) on the gas pressure is shown. One can see that the ZDW can be tuned from 700 to below 500 nm by varying the pressure from 2.5 atm to 0.25 atm.

For the numerical simulations we use a generalized version of the propagation equation for the electric field strength E of forward-going waves [8, 15]

$$\frac{\partial E(z,\omega)}{\partial z} = i\left(\beta(\omega) - \frac{\omega}{c}\right)E(z,\omega) - \frac{\alpha(\omega)}{2}E(z,\omega) + \frac{i\omega^2}{2c^2\epsilon_0\beta_j(\omega)}P_{NL}(z,\omega) \quad (1)$$

where P_{NL} describes the nonlinear Kerr polarization as well as the photoionization-induced nonlinear absorption and phase modulation by the plasma, and z is the axial coordinate (for details see [15]). This equation does not rely on the slowly-varying envelope approximation, includes dispersion to all orders, and can be used for the description of extremely broad spectra. Since the transfer to higher-order transfer modes is small, we consider only the fundamental linearly-polarized HE_{11}-like mode. The nonlinear refractive index of argon is $n_2 = 1 \times 10^{-19}$

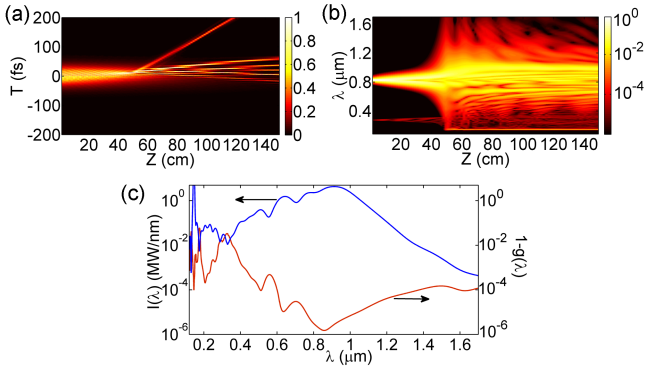

FIG. 2: High-power and high-coherence optical supercontinuum generation in a kagome-lattice HC-PCF filled with argon at 0.25 atm. In (a) the evolution of the temporal profile and in (b) the spectral evolution for an input 50-fs pulse at 800 nm with a peak intensity of 176 TW/cm^2 are presented. In (c) the output spectrum (blue upper curve) and the coherence function (red lower curve) after 60 cm propagation are presented. The other parameters are as in Fig. 1.

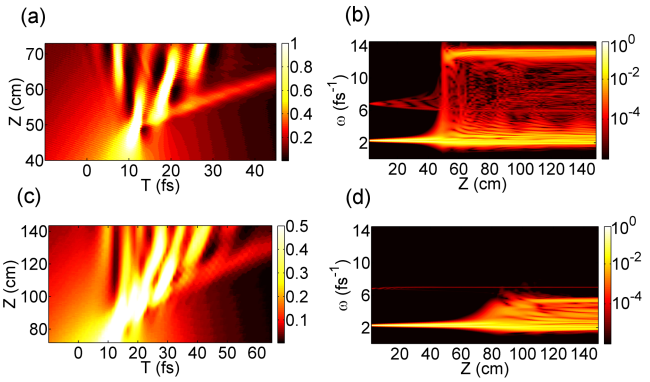

FIG. 3: Temporal and spectral evolution of generated radiations in the kagome lattice HC-PCF filled with argon at different pressures. The input 50 fs pulse at 800 nm has the peak intensity of 176 TW/cm^2 for a pressure of 0.25 atm (a),(b) and 14 TW/cm^2 for a pressure of 2 atm (c),(d).

cm^2/W/atm. Besides the spectral and temporal properties, the coherence of the SC is of crucial importance for most applications. We study the first-order coherence function $g(\lambda)$ [12] which directly corresponds to the visibility measured in interference experiments. The effect of quantum noise is included by adding to the input field the shot quantum noise in the approach of the Wigner quasi-probability representation [16].

The evolution of the temporal shape presented in Fig. 2(a) can be divided into three stages: (i) the strong initial compression, (ii) formation of a high-order soliton with periodic modulations of the intensity, and (iii) the final splitting into several fundamental solitons. After 50 cm of propagation, besides the longitudinally modulated trace of a higher-order soliton, one can see a separate diverging trace. The presence of higher-order dispersion leads to a transfer of energy from the high-order soliton to narrow-band resonant non-solitonic radiation (NSR) in the normal GVD region, the position of this resonance is determined by the phase-matching condition [8] which is the same as for the fundamental soliton. In contrast to solid-core PCFs, here the absent Raman effect and low third-order dispersion coefficient result in the stability of the high-order soliton over a considerable length. This soliton-related dynamics explains the spectral evolution as presented in Fig. 2(b). At the first stage of evolution the combined effect of nonlinear phase modulation and anomalous dispersion results in a dramatic spectral broadening at around 50 cm (so-called soliton compression) and the formation of a high-order soliton. With further propagation, on the long wavelength side a periodic modulation arises. The spectrum at the optimum propagation length of 60 cm is shown in Fig. 2(c) and cover more than two-octave broad range from 150 to 1300 nm. The spectral peak power density reaches high values up to the range of MW/nm which is by five orders of magnitude higher than achieved previously in solid-core PCFs. In the red lower curve of Fig. 2(c) we present the incoherence $1 - g(\lambda)$ of the supercontinuum, which is caused by the influence of quantum noise. It can be seen that the coherence function $g(\lambda)$ is close to unity over the whole spectral range, with the average spectrum-weighted value of $\overline{g(\lambda)} = 1 - 10^{-4}$. The high coherence is explained by the relatively low soliton number $N \sim 10$; higher values of the soliton number typically lead to a significant degradation of the coherence [12]. In a kagome-lattice HC-PCF the soliton number, and therefore the output coherence, for the same input pulse parameters can be controlled by the variation of the pressure.

An interesting physical phenomenon in Fig. 2(a) is connected with the bright trace diverging at a large angle which appears in the spectrum in Fig. 2(b) as the narrow-band bright trace at 150 nm. This isolated short-wavelength peak can be understood as arising by the emission of NSR by the short-lived maximum-bandwidth stage of the high-order soliton. At this stage, the overlap of the soliton spectrum with the resonance frequency is maximal. This is more clearly seen in the enlarged scale in Fig. 3(a) or in the evolution of spectrum in Fig. 3(b) which is shown for clarity as a function of frequency (the parameters are the same as in Fig. 2). In the first stage only the pump at 2.26 fs^{-1} and its third harmonic at 6.8 fs^{-1} can be seen, but after 50 cm an intense band in the high-frequency region at 13 fs^{-1} (corresponding to 150 nm) is visible. The duration of the NSR peak is determined by a group velocity mismatch between the high-order soliton and the NSR and on the other hand, a propagation distance over which the soliton spectrum overlaps with the resonance frequency.

One can see in Fig. 2(a) and 3(a) that the NSR pulse is generated only as long as the soliton is strong enough and therefore broadband enough to provide seed components at the NSR frequency. With further propagation, after roughly 3 cm the periodic modulation typical for a higher-order soliton leads to a reduction of the overlap and a disconnection of the soliton spectrum with the resonance frequency, and the generation of NSR stops, resulting in a NSR pulse duration below 10 fs. Careful examination of Fig. 3 reveals that the broadband soliton stage exists over roughly 3 cm, which in connection with the group velocity mismatch of $6\times10^{-5}c$ leads to a NSR pulse duration of 6 fs, in correspondence with the numerical observations. The above origin of the UV/VUV spectral components can be checked by the study of the phase-matching condition. In the solid (red) line in Fig. 1(d), the phase-matched wavelength for the emission of NSR in dependence on the argon pressure is presented. As can be seen, assuming a soliton at 800 nm, the position of the resonance is at 150 nm for a gas pressure of 0.25 atm. The position of the phase-matched wavelengths can be continuously tuned to longer wavelengths with increasing pressure. To examine this prediction further, in Fig. 3(c),(d) the spectral and temporal evolution of a 50-fs pulse at 800 nm for a pressure at 2 atm is presented. The peak intensity here is only 14 TW/cm^2 and the bright high-frequency narrow band at 5 fs^{-1} (or 350 nm) is emitted at the wavelength corresponding the phase-matching condition for 2 atm as given in Fig. 1(d). Note that the described emission of an ultrashort VUV pulse can not be achieved in solid-core PCFs, where the extension of spectra below 350 nm is impeded by loss in the VUV and much stronger dispersion which modifies the fission dynamics and the energy transfer to the NSR.

To study the emission of the bright UV/VUV component further, in Fig. 4(a) the temporal shape of the electric field at a pressure of 0.25 atm after 105 cm propagation is presented. At this distance the bright UV/VUV component with central wavelength at 150 nm is clearly separated from the rest of the pulse, its duration (FWHM) is only 5 fs and it exhibit about the same maximum intensity as the input pulse. The energy of this ultrashort VUV pulse is about 25 μJ or 20% of the input pulse energy. The central frequency of the UV/VUV pulses can be simply tuned by the change of the pressure. As can be seen in Fig. 4(b) with decreasing pressure the high-frequency spectral peak is tuned to shorter wavelengths; for 2 atm the UV/VUV component is at 350 nm, for 1 atm at 250 nm, for 0.5 atm at 180 nm and for 0.25 atm at 150 nm. For still lower pressures the wavelength can be reduced up to 115 nm. Note that in the different curves of Fig. 4(b) different input intensities has been chosen, but the fraction of energy in the UV/VUV part is always about 20% while the pulse durations vary from 5 fs for 0.25 atm to 20 fs for 2 atm, due to different group velocity mismatch at different UV/VUV frequencies.

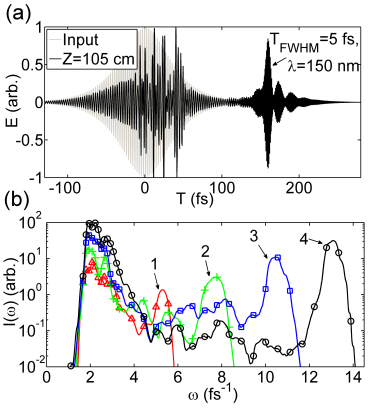

FIG. 4: Pulse shape (a) and tunable UV/VUV spectra for different pressures (b). In (a) the electric field strengths for a pressure of 0.25 atm are presented. Here, the gray solid represents the 50-fs input pulses at 800 nm and the black one the electric field strength after propagation of 105 cm. In (b) the spectra after propagation of 120 cm of the input 50-fs pulse at 800 nm at pressure of 2 atm and intensity of 14 TW/cm^2 (red curve 1), 1 atm and 35 TW/cm^2 (green curve 2), 0.5 atm and 88 TW/cm^2 (blue curve 3) and 0.25 atm and 176 TW/cm^2 (black curve 4) are presented.

In conclusion, we propose to use kagome-lattice HC-PCFs filled with a noble gas for the generation of high-power supecontinua and sub-10-fs pulses tunable by the pressure over a broad UV-VUV range. These predictions should be interesting for many applications and can bring qualitative advances in several fields. To remark a few: high power SC sources can replace several lasers at different frequencies (including frequencies where lasers do not exist), it can increase the detection sensitivity in nonlinear spectroscopic methods such as CARS spectroscopy and bio-medical microscopy and spectroscopy, and it can lead to advances in high-resolution frequency comb spectroscopy. On the other hand, the prediction of a novel method for tunable sub-10-fs VUV pulses with energy in the μJ range could improve the pulse parameters accessible ultrafast time-resolved measurements in physics, chemistry, biology and other fields.

We acknowledge financial support from the German Academic Exchange Service (DAAD) and the German Research Foundation (DFG).

[1] P. St. J. Russell, Science **299**, 358 (2003).
[2] R. F. Cregan *et al.*, Science **285**, 1537 (1999).
[3] F. Benabid, J. C. Knight, G. Antonopoulos, and P. St. J. Russelll, Science **298**, 399 (2002).
[4] F. Couny, F. Benabid, and P. S. Light, Opt. Lett. **31**, 3574 (2006).
[5] F. Couny, F. Benabid, P. J. Roberts, P. S. Light, and M. G. Raymer, Science **318**, 1118 (2007).
[6] S. J. Im, A. Husakou, and J. Herrmann, Opt. Express

17, 13050 (2009).
[7] J. K. Ranka, R. S. Windeler, and A. J. Stentz, Opt. Lett. **25**, 25 (2000).
[8] A. V. Husakou and J. Herrmann, Phys. Rev. Lett. **87**, 203901 (2001).
[9] J. Herrmann *et al.*, Phys. Rev. Lett. **88**, 173901 (2002).
[10] J. M. Dudley *et al.*, Opt. Express **12**, 22423 (2002).
[11] A. Ortigosa-Blanch, J. C. Knight, and P. St. J. Russell, J. Opt. Soc. Am. B **19**, 2567 (2002).
[12] J. M. Dudley, G. Genty, and S. Coen, Rev. Mod. Phys. **78**, 1135 (2006).
[13] K. Kosma, S. A. Trushin, W. E. Schmid, and W. Fu, Opt. Lett. **33**, 723 (2008).
[14] P. Tzankov *et al.*, Opt. Express **15**, 6389 (2007).
[15] A. Husakou and J. Herrmann, Opt. Express **17**, 12481 (2009).
[16] P. D. Drummond and J. F. Corney, J. Opt. Soc. Am. B **18**, 139 (2001).